J Mater Sci (2025) 60:10467–10477

Materials for life sciences

Utilising design of experiment to design an optimised bioink for 3D bioprinting

Alice Upton[1], Athina Mylona[2], and Georgina Zimbitas[1,*]

[1] *Institute of Medical Science, Canterbury Christ Church University, North Holmes Road, Canterbury CT1 1QU, UK*
[2] *Kent and Medway Medical School, Park Wood Road, Pears Building, Canterbury CT2 7FS, UK*

Received: 7 March 2025
Accepted: 31 May 2025
Published online: 20 June 2025

ABSTRACT

The advancement of bioinks for 3D bioprinting is vital for tissue engineering, requiring precise tailoring of rheological and structural properties. This study employs integration of rheological analysis with a design of experiment (DoE) approach, with the aim being the optimisation of bioink formulations comprising of hyaluronic acid, sodium alginate, and dextran-40. A factorial DoE identified sodium alginate as the primary determinant of the bioinks' viscosity, while the mixture DoE established an optimal formulation with a viscosity of 3.275 Pa·s, matching the viscosity of the commercial benchmark. Rheological assessments confirmed the optimised bioink's shear-thinning properties and structural integrity, essential for printability and cellular support. Capability analysis of multiple batches demonstrated process reliability, whereby viscosities were consistently within defined boundaries, emphasising the robustness of the DoE-guided formulation process. This research highlights the potential of combining statistical and rheological methodologies to develop bioinks tailored for specific tissue applications, paving the way for improved 3D bioprinting outcomes.

Introduction

The groundbreaking research by Langer and Vacanti [1] introduced the foundational concept of combining cells, biodegradable scaffolds, and biological signals to engineer functional tissues and organs, establishing tissue engineering as a significant and influential scientific discipline. In tissue engineering cells are viewed as building blocks, or even more so as factories that produce matrices for structural tissues, e.g. connective tissues [2, 3]. Further development in the field introduced scaffolds that structurally support cells undergoing maturation, with cells seeded on a scaffold [4]. Recently, advances in 3D bioprinting have allowed printing of bioinks containing living cells within a hydrogel composition. The development of bioinks suitable for maintaining live cells during the printing process continues to play a pivotal role in 3D bioprinting; these bioinks need to provide a supportive environment for encapsulated cells, facilitating their viability, proliferation, and differentiation within the printed constructs [5,

Handling Editor: Steven Naleway.

Address correspondence to E-mail: georgina.zimbitas@canterbury.ac.uk

https://doi.org/10.1007/s10853-025-11076-1

6]. Bioinks must possess several key characteristics to effectively mimic the native extracellular matrix of the target tissue [7], including biocompatibility [8], printability [9], bioactivity [10], and mechanical properties tailored to the specific tissue type and applications [11, 12].

The wide range of applications for bioinks means that composition of bioinks would also vary to ensure the aforementioned desired properties of the printed tissue construct are met [13]. Typically, bioinks consist of a combination of biomaterials that stimulate cell proliferation and growth. Such materials include natural polymers (e.g. alginate [14], collagen [15], gelatin [16], hyaluronic acid [17]) and/or synthetic polymers (e.g. polycaprolactone [18], polyethylene glycol [19]) that provide the structural framework and biochemical cues necessary for cell adhesion, proliferation, and tissue development. Additional components (e.g. methyl acrylamide) are included to improve stiffness and structural integrity of the bioink [20].

For extrusion-based printing, optimal printability of 3D bioinks includes careful tuning of multiple interdependent factors to ensure high fidelity, viability, and functionality of the printed biological constructs. These include printing parameters, such as nozzle diameter and extrusion speed, environmental conditions, such as temperature, and bioink mechanical properties, which include rheological behaviour of the bioink. In the case of mechanical properties, the bioink must be able to exhibit shear-thinning behaviour, whereby its viscosity under shear for extrusion is low enough to allow easy printing, but high enough at rest to maintain the printed shape. Combining all these parameters to develop and optimise bioinks for extrusion-based 3D bioprinting presents with significant challenges and opportunities in tissue engineering, with the mechanical properties of bioinks being crucial for successful 3D bioprinting.

For printability of 3D bioinks, rheological characterisation is often utilised to examine key mechanical properties [21–23] including dynamic viscosity (hereon after referred to as viscosity), which affects flow behaviour during printing, and shear-thinning behaviour, enabling easier extrusion through printing nozzles [24]. By optimising these properties through formulation and processing, bioinks can be tailored to not only be printable, but to also maintain their ability to mimic native tissue structures and support cell viability, proliferation, and tissue regeneration within printed constructs [25].

It is the integration of rheology and design of experiments (DoE) statistics, however, that truly offers the opportunity of a systematic approach for optimising bioink formulations. Whereas rheology characterises bioink properties, such as viscosity and shear-thinning behaviour [26], DoE provides a methodical platform to explore the bioink's characterisation and identify optimal conditions, such as material concentrations and printing pressures, within controlled parameters, while also minimising the number of trials needed to obtain targeted results [27].

Viscosity and shear-thinning behaviour are critical to determining material printability and, as such, are the rheological focus of this paper, whereby a study is presented that combines Rheology and DoE methodologies to investigate the development of a bioink for soft tissue 3D printing. The emphasis here is on obtaining tailored viscosity and shear-thinning properties to enhance printability and structural integrity.

Methods and materials

Preparation of biomaterials

Materials

Bioink samples were prepared using hyaluronic acid (Biosynth, UK, Molecular Weight: 1-2million Daltons), dextran-40 (Thermo Scientific, UK), phenol-free DMEM (Gibco, UK) supplemented with 5% human platelet lysate (HPL) (Stem Cell Technologies, UK), and sodium alginate (Thermo Scientific, UK, Molecular Weight: 12,000–40,000 Daltons). Supplier specifications for the alginate were 60–70% mannuronic acid and 30–40% guluronic acid.

Bioink samples preparation

Samples were prepared according to the Minitab® 21 DoE Mixture output (See Supplementary Information). Each sample component (see section "Design of Experiment (DoE)") was weighed out to the desired concentration (w/v%) and UV-sterilised in a UV-clave for 15 min. Final samples were manually mixed between two Luer-Lock syringes for 10 min to ensure complete homogenisation. An Invitrogen M5000 optical microscope, visualised under brightfield at ×10 magnification, was used to confirm absence of phase separation

and clumping, thereby verifying the homogenisation of the sample.

Design of Experiment (DoE)

Factorial DoE

A full factorial DoE in Minitab® 21 was implemented to generate a 2-level design DoE as described by Heathman et al. [28]. The DoE contained upper and lower constraints for three components, referred to as factors throughout: hyaluronic acid (HA), sodium alginate (ALG), and dextran-40 (DEX). The remainder of the mixture was made up of phenol-free DMEM media. The outputs of the DoE produced nine sample combinations (see Supplementary Information). In accordance with Petta et al. [29], Schmid et al. [30], and Zidarič et al. [31], the concentration limits for each factor were set as shown in Table 1.

Mixture DoE

Minitab® 21 was also used to format a 4-factor mixture DoE, generating an extreme vertices design that allows for sub portions of the upper and lower limits of each factor to be considered. The same three factors used in the factorial DoE are used here, with phenol-free DMEM media now also being added as a factor. The output of the DoE generated 35 sample combinations of the 4 components (See Supplementary Information), using concentrations (w/v%) within the same concentration limits applied in the factorial DoE (Table 2).

Table 1 DoE concentration limits for the three factors used (factorial DoE)

Mixture component	Concentration limits (w/v%)	
	Lower constraint	Upper constraint
Hyaluronic Acid	0.5	2.0
Sodium Alginate	0.5	5.0
Dextran-40	0.5	2.0

Formulation of optimised bioink

Mixture DoE data were submitted into the Response Optimiser of Minitab® 21 to define the most statistically accurate concentration (w/v%) for each factor, with the desired viscosity target. CELLINK SKIN Bioink (CELLINK, UK) was used as a reference bioink, and its viscosity of 3.275 Pa·s at 25 °C was used as the target viscosity in the Response Optimiser. Upper and lower boundaries of 10% from the target were used, set at 3.602 Pa·s and 2.945 Pa·s, respectively.

Quality assessment of development process

The optimised formulated bioink was prepared in ten individual batches and subjected to an isothermal temperature test for DoE (see section "Isothermal Temperature Test for DoE"). A Levene's equal variance test ($p < 0.05$) was applied to the viscosity data to test for equal variances, whereas an Anderson–Darling normality test ($p > 0.05$) was applied to test for normal distribution within the data. Finally, the viscosity data were inputted into the capability analysis tool of Minitab® 21 to evaluate the development process, using the target viscosity of 3.275 Pa·s and the same upper and lower specifications of 10%. Overall and potential capability values produced are shown in the results section "Quality assurance of the bioink development".

Table 2 DoE concentration limits for the four factors used (mixture DoE)

Mixture component	Concentration limits (w/v%)	
	Lower constraint	Upper constraint
Hyaluronic Acid	0.5	2.0
Sodium Alginate	0.5	5.0
Dextran-40	0.5	2.0
Phenol-Free DMEM culture media	Limit automatically calculated as remainder or the addition of the above concentrations	

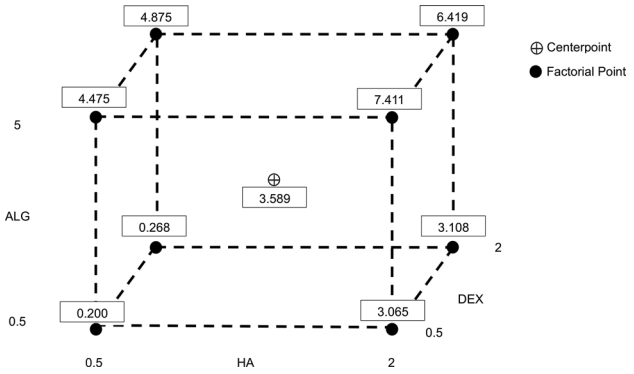

Figure 1 Cube Plot of a 3 component bioink. The plot depicts upper, midpoint, and lower viscosities (in Pa.s) relative to the concentration (in w/v%) of each of the bioinks' three components: hyaluronic acid (HA), sodium alginate (ALG), and dextran-40 (DEX). Factorial points identify the upper and lower percentage limits used within the Factorial DoE. The centrepoint identifies the mid viscosity at the mid percentage point of each factor. Nine samples were rheologically tested in triplicates, with the centrepoint sample tested in two sets of triplicates

Rheometer

An Anton Paar MCR 92 rheometer was used to perform rheological tests, and resulting data were collected through the RheoCompass 1.30 software. The methodology has been adapted from Cavallo et al. [32] and is as follows: A parallel plate geometry of 25 mm was employed. 1 ml of the sample was added to the rheometer for testing. The geometry was lowered to a zero-gap of 1 mm, and the excess sample was carefully removed. Test details are described below.

Isothermal temperature test for DoE

This rotational test was performed to determine the viscosity of the sample at a constant temperature of 37 °C, replicating human body temperature. Viscosity and shear stress were measured as a preset function of shear rate. During the test, the sample was held at a temperature of 37 °C for 1 min. The sample was preshearred at a shear rate of 10 s^{-1} for 1 min. Finally, the sample was sheared at a high shear rate of 80 s^{-1} for 2.5 min.

Flow curve

This rotational test was performed to determine the material's viscous flow behaviour. The flow curve was programmed with a preset shear rate. The linear ramp of the shear rate was set to increase from 1 to 100 s^{-1} in increments of 1 s^{-1}. The temperature was preset to the desired temperature of either 25 °C or 37 °C, dependent on the sample.

Statistical analysis

All statistical analyses were performed using Minitab® 21. Parametric statistical analysis was performed after the appropriate test assumptions were met, for both the normality test (Anderson–Darling) and the equal variance test (Levene's test). Data significance was determined using the biological probability threshold of 0.05 with a 95% confidence prediction.

Results

Factorial DoE

To examine the effects of the individual components on the bioinks' composition and physical behaviours, a full factorial DoE was generated using Minitab® 21. The factors used were the 3 bioink components: hyaluronic acid (HA), sodium alginate (ALG), and dextran-40 (DEX).

Viscosity data obtained from the full factorial DoE are represented in a Cube Plot (Fig. 1), which visually

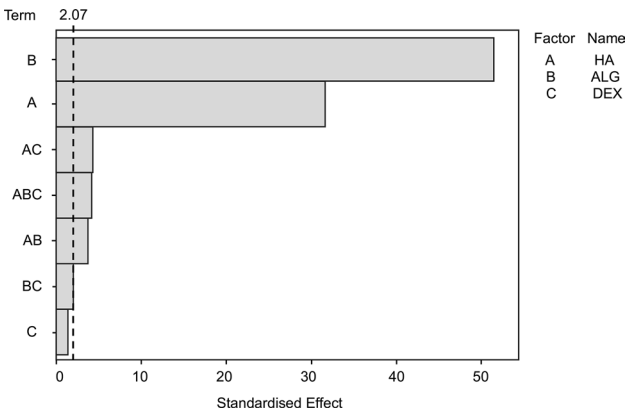

Figure 2 Pareto Chart of standardised effects of each of the factors on the final bioink composition. The 3-factor bioink mixture is composed of: hyaluronic acid (HA), sodium alginate (ALG), and dextran-40 (DEX). The reference line of statistical significance (shown here as a dashed line) was set at 2.07 (1 minus the confidence level for the analysis), with any factor that crosses this line indicating a significant effect towards the viscosity of the bioink ($P > 0.05$). Nine samples were rheologically tested in triplicates, with the centrepoint sample tested in two sets of triplicates

represents the effects of the three bioink factors on viscosity, thus helping in understanding how viscosity changes across the various combinations of factor concentrations. In the Cube Plot, a low viscosity of 0.200 Pa·s, a midpoint viscosity of 3.589 Pa·s, and a high viscosity of 7.411 Pa·s are identified.

Furthermore, a Pareto Chart (Fig. 2) was employed to identify the significance of factors on the bioinks' viscosity. For this, the magnitude of the effects of the three different factors and their interactions on viscosity was ranked, in ascending significance. The data presented (Fig. 2) show ALG most significantly effects viscosity, followed by HA, whereas DEX appears to have no significant effect on bioink viscosity.

Mixture DoE—optimisation of bioink

Minitab® 21 was used to format a mixture DoE to develop a reliable and printable bioink. The DoE was represented as an extreme vertices diagram and was designed to incorporate upper and lower bound constraints (w/v%) of each component (factor) of the bioink: hyaluronic acid (HA), sodium alginate (ALG), and dextran-40 (DEX), with phenol-free DMEM supplemented with 5% HPL. The DoE also included varying concentration ranges of each factor of the bioink, while ensuring that the total composition was always equal to 100%. Experimental samples were then prepared, all in accordance with the Minitab DoE output, and measured for their rheological behaviour, in accordance with the Minitab® 21 generated sample run list (see Supplementary Information).

CELLINK SKIN was utilised as a reference for viscosity in producing a bioink, as a commercial bioink provides established benchmarks for properties like viscosity, biocompatibility, and printability, offering clear performance targets. CELLINK SKIN Bioink was measured at a target viscosity of 3.275 Pa·s at 25 °C, as stated by the manufacturer, which is where the viscosity of this bioink begins to plateau under increasing shear rate (Fig. 3). The flow curve showed the viscosity began to plateau at a shear rate of 80 s^{-1}, with the rheological assumption that the optimised bioink will present similar flow and deformation with increasing force applied.

The output samples generated by the mixture DoE were then subjected to the same shear rate of 80 s^{-1}, to compare rheological behaviour with that displayed by the CELLINK SKIN reference bioink. The viscosity of each sample inputted in the DoE was generated from

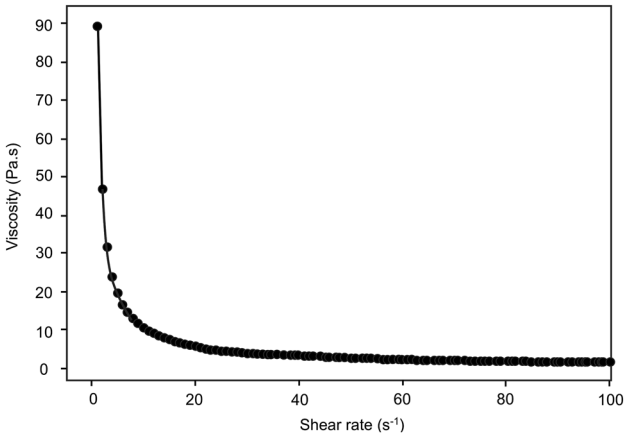

Figure 3 Flow Curve of CELLINK SKIN. The reference bioink CELLINK SKIN was subjected to an increasing shear rate from 1 to 100 s^{-1}, increasing by 1 s^{-1} every 2 s at a constant temperature of 25 °C. The curve shows viscosity beginning to plateau at a shear rate of 80 s^{-1}

the isothermal temperature test performed at a constant shear rate of 80 s^{-1} and at a temperature of 37 °C. The DoE data output was then subjected to statistical optimisation using the response optimiser in the mixture DoE of Minitab® 21, which is standard operation when evaluating multi-response outputs from a DoE run [33]. The mixture DoE produced a series of bioink compositions with one having a 100% match to the target viscosity of 3.275 Pa·s. This w/v% composition comprised of 1.25% hyaluronic acid, 2.52% of sodium alginate, and 0.50% of dextran-40 (Fig. 4).

Quality assurance of the bioink development

Performing a normal capability analysis serves as a critical tool to evaluate the process of bioink development using rheological behaviour and the DoE approach. This analysis assesses whether the bioink development process consistently produces outputs — in this case, viscosity — that meet the desired target specifications. By quantifying the alignment of process outputs with predefined criteria, capability analysis ensures that the DoE approach is effectively optimising the formulation and processing parameters.

Furthermore, capability analysis identifies variations within the development process, offering insights into areas where the process can be refined. For instance, an analysis where results reveal the process is only marginally meeting the target range

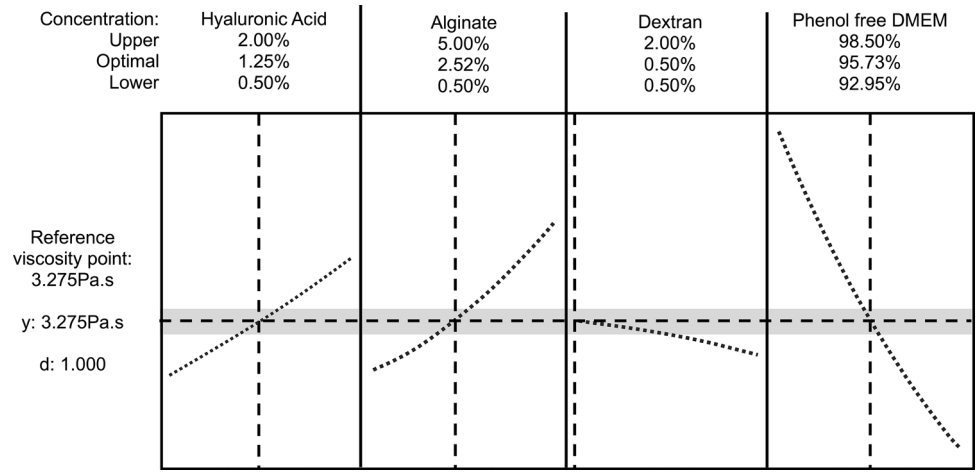

Figure 4 Response Optimisation of Bioink designed by the Mixture DoE. For each sample, the DoE outputs were input into the response optimiser of Minitab® 21. The input target viscosity of 3.275 Pa·s was used, and a ±10% boundary was set, which is shown as the horizontal shaded area in the graph. The dashed horizontal line represents the target viscosity (Pa.s). Solid vertical lines demonstrate boundaries of the individual factors, whereas dashed vertical lines represent the optimal concentration of each factor. The result was an optimal w/v% concentration comprising of 1.25% HA, 2.52% ALG, 0.50% DEX, and 95.73% DMEM (supplemented with 5% HPL). y: predicted response (viscosity), d: desirability value, here being 1 and thus indicating the predicted viscosity (y) for the suggested composition is 100% in agreement with the target viscosity

or has a high degree of variability can indicate a need to enhance other factors, such as material selection, crosslinking methods, or mixing protocols. This proactive approach helps in maintaining consistent quality while reducing batch-to-batch variability.

The capability analysis also evaluates the robustness of the process, ensuring that the bioink can reliably perform under different conditions without compromising functionality. By integrating capability analysis into bioink development, this can systematically improve the process, align outputs with application-specific requirements, and ensure that the final bioink formulation meets high standards of performance and reproducibility.

As mentioned previously, the viscosity of the reference CELLINK SKIN Bioink at 25 °C was used as the target viscosity, 3.275 Pa·s, and upper and lower boundaries of 10% from the target were set, here being at 3.602 Pa·s and 2.947 Pa·s, respectively. The normal capability analysis was performed on ten independent experimental batches of the final bioink composition generated by the mixture DoE. An isothermal temperature test (as described above) was performed 10 times to produce 10 readings for each of the sample and CELLINK SKIN batches, with Fig. 5 representing the average viscosity of the ten measurements for each of these batches. The results show minimal variability across the majority of the batches, with none of the samples exceeding the predefined upper or lower limits. Batches 3, 9, and 10 exhibit the highest viscosities, approximately 3.300–3.325 Pa·s, compared to the reference bioink's viscosity of approximately 3.250 Pa·s. Batches 1, 2, 4, 7, and 8 have viscosities close to the reference, indicating they are comparable to CELLINK SKIN. Batches 5 and 6 show lower viscosities, with Batch 5

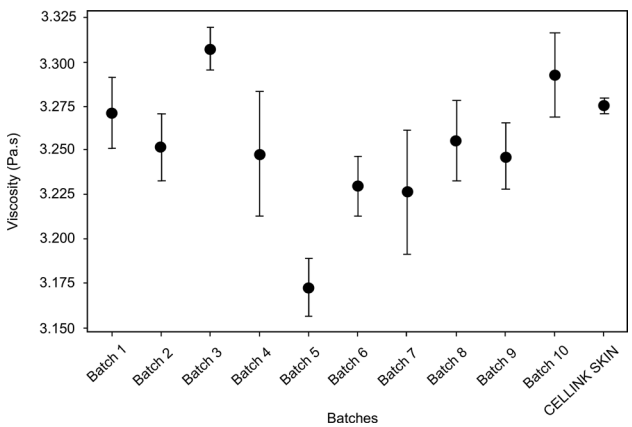

Figure 5 Average viscosity for 10 batches of optimised ink. For each batch, the isothermal temperature test of the rheometer was used to take ten viscosity measurements that were then averaged and plotted. The test was operated at a constant temperature of 37 °C and a constant shear rate of 80 s^{-1}

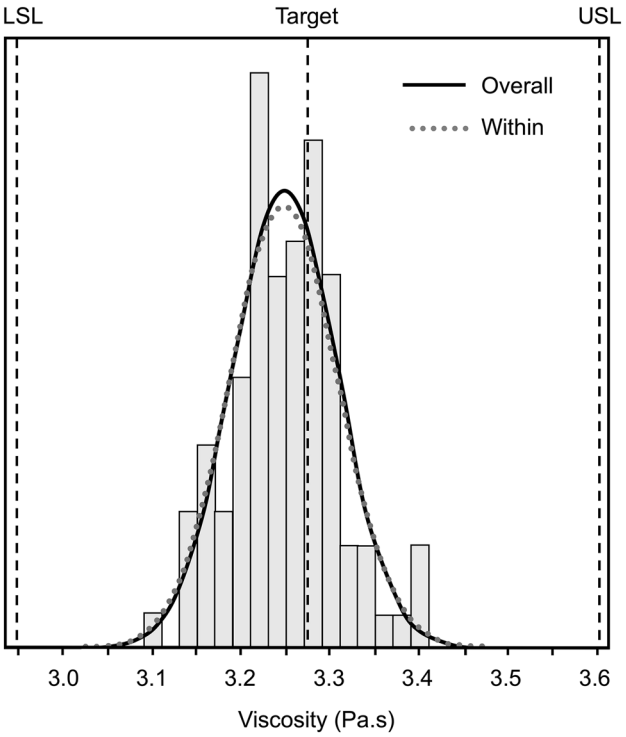

Figure 6 Capability Histogram Analysis. The histogram and fitted curves (for 'Overall' and 'Within' analysis) illustrate the distribution of process data relative to the lower specification limit (LSL), upper specification limit (USL), and the target viscosity value of 3.275 Pa.s. The actual spread is represented by 6 sigma

being the least viscous at about 3.175 Pa·s. The sample mean viscosity was determined as 3.249 Pa·s, with overall standard deviation of 0.059 Pa·s, while the within-batch standard deviation was 0.061 Pa·s.

Figure 6 presents the histogram output of the normal capability analysis, and Table 3 shows the results of this analysis. These results are split into two categories: "overall" referring to overall variations, e.g. variations within batches, across batches, etc., and "within" referring to variations occurring solely within each individual batch. The specified limits of the normal capability analysis refer to the constraints applied to the target viscosity of 3.275 Pa·s and the ±10% boundary limit set, described as lower and upper specification limits.

For results of the overall analysis of the normal capability analysis, the process capability (Pp) is a measure of the overall capability of the process, comparing the overall process spread (total variation, including between and within batches) to the specification limits, here being specified by the viscosity target. The obtained Pp ratio of 1.85 suggests a relatively small spread compared to the width of the specification limits. Any Pp ratio larger than 1.5 indicates that the bioink production is well within the specified limits of the ±10% boundary of the target viscosity of 3.275 Pa·s.

The Lower and Upper Process Performance Indexes (PPL and PPU, respectively) are compared to the lower and upper specification limits of the viscosity target to see how well the lower and upper sides of the process distribution fit within the specification limits. The obtained PPL and PPU value of 1.70 and 1.99, respectively, are both higher than 1, indicating the lower and upper tails of the process variability lie comfortably within their respective limits. Therefore, it can be concluded that obtaining values outside of these limits is unlikely.

The Process Performance Capability Index (Ppk) takes into consideration not only the overall variability within the process, but also how well the process in centred considering the defined limits of the viscosity target. The obtained Ppk value of 1.70 implies the process generates a bioink with viscosity that lays inside the target boundaries and also implies an unlikelihood of the process producing a bioink viscosity that is out of the target boundary. As the name suggests, the Process Capability Index Centred on the Target (Cpm) considers how well the process is centred around a defined target (here being the target viscosity of 3.275 Pa.s). A Cpm value of 1.70 confirms the

Table 3 Results of the capability histogram analysis, including outputs for both "Overall" and "Within" analysis

Process data (Pa.s)		Capability	Overall		Within	
Lower Specification Limit (LSL)	2.947	Lower Index	PPL	1.70	CPL	1.64
Upper Specification Limit (USL)	3.602	Upper Index	PPU	1.99	CPU	1.93
Target Viscosity	3.275	Capability	Pp	1.85	Cp	1.79
Sample Mean	3.249	Capability Index	Ppk	1.70	Cpk	1.64
Number of Samples, N	100	Standard Deviation (Pa.s)		0.059	0.061	
		Process Capability Index Centred on the Target			Cpm	1.70

findings from the previous overall capability indexes, in that it concludes that this is a capable and well-centred process.

The results for the within capability analysis are in-line with those obtained for the overall capability analysis. The Potential Capability Index (Cp) compares within-batch variations, while ignoring batch-to-batch variabilities. The obtained Cp value of 1.79 indicates a controlled within-batch variability between the bioinks. This, in turn, concludes the bioink development process is reliable, in that it can produce consistent results obtaining the targeted viscosity, while remaining inside the viscosity boundaries. The Lower and Upper Capability Indexes (CPL and CPU) resemble the PPL and PPU seen in the overall capability analysis; however, the distribution among batch variations is considered. These batch viscosities were compared to the lower and upper specification limits seen before for PPL and PPU. The CPL and CPU values of 1.64 and 1.93, respectively, indicate that the batch viscosity lays inside the target viscosity boundaries.

The within analysis CPL value is slightly lower than the respective overall analysis PPL value, indicating that within-batch variation may be more significant than overall variability. For upper boundaries, the CPU value closely resembles that of the PPU, indicating good overall control on the upper side of the variability distribution. For the "Within" process, a capability index (Cpk) value of 1.33 is considered satisfactory [34], whereas anything above 1.5 is regarded as very good. Obtained here is a Cpk value of 1.64, which concludes a capable process. This value is, however, slightly lower than the overall analysis Cp value of 1.79, which can imply that the process is slightly off-centre and closer to the LSL limit. A comparison of the Cpk and Ppk values indicates that the overall process variability is marginally better than the within-batch variability, something not commonly seen. Overall, the conclusion is that the process is stable long-term and is consistent across batches, represented by the six-sigma spread.

Discussion

The primary focus in this study was to develop a bioink with rheological properties specifically optimised for extrusion-based 3D bioprinting. These rheological properties focussed on viscosity and shear-thinning behaviour as they are the critical determinants of printability, influencing both flow through the nozzle and the structural fidelity of the printed construct. As such, viscosity was selected as the primary response variable within the design of experiment (DoE) approach, to enable systematic optimisation with minimal experimental complexity.

The application of design of experiment (DoE) statistical tools in the development of bioinks for 3D bioprinting represents a significant advancement in the field of tissue engineering. By utilising this systematic approach, DoE allows the efficient optimisation of bioink formulations that need meet specific criteria. In this study, we have employed the DoE to determine the viscosity effects of three factors—hyaluronic acid (HA), sodium alginate (ALG), and dextran-40 (DEX)—focussing on viscosity, thereby aiming to produce an optimised bioink suitable for soft tissue applications.

The DoE approach allowed for a comprehensive analysis of the effect of varying concentrations of the three bioink factors on the bioink's physical properties. The factorial DoE revealed that sodium alginate had the most significant impact on increasing viscosity, followed by hyaluronic acid, whereas dextran-40 showed no significant direct effect on viscosity. This insight was critical in formulating a bioink that not only met the target viscosity but also exhibited desirable shear-thinning behaviour, which is crucial for printability. The optimised w/v% bioink composition, identified through mixture DoE, consisted of 1.25% hyaluronic acid, 2.52% sodium alginate, and 0.5% dextran-40, all in a phenol-free DMEM media supplemented with 10% HPL, achieving the target viscosity of 3.275 Pa·s.

Ensuring consistency and reliability in bioink production is paramount for successful 3D bioprinting. The capability analysis carried out on individually produced batches of the optimised bioink showed that, while most batches fell within the specified viscosity range, some variability was present in viscosity; however, this variation remained within the viscosity boundaries. This variability underscores the need for stringent quality control measures to minimise batch-to-batch variation and ensure synthesis reproducibility. Capability indices were used to assess the process' potential capability to produce bioinks within the desired specifications. The results indicated that the current process is capable, but further refinement is needed to enhance consistency via narrowing the boundaries of the target viscosity.

The successful application of DoE in optimising bioink formulations demonstrates its potential as a powerful tool in tissue engineering. This study's findings provide a framework for developing bioinks with tailored properties, ensuring that they meet the specific requirements for different tissue types. Moreover, this study highlights the importance of continuous quality control and process optimisation in bioink development. Establishing standardised benchmarks for quality assessment, such as the CpK value, can help to ensure that bioinks consistently meet the desired criteria. As the field of bioprinting advances, the integration of advanced statistical tools like DoE with rheological and mechanical characterisation will be essential in developing the next generation of bioinks capable of supporting complex tissue regeneration and repair.

While other mechanical properties, e.g. elastic, storage, and loss moduli, provide valuable information about the post-print structural and mechanical integrity of hydrogels, these parameters were outside the scope of our current optimisation, which was focussed on flow behaviour during the printing phase rather than post-gelation mechanics. While this study focussed on the evaluation of flow characteristics essential to printability, it does not capture other parameters, such as gelation kinetics, cell compatibility, or the mechanical integrity of the printed construct post-printing. In future iterations, incorporating additional response variables — such as elastic, storage, loss moduli, and cell viability metrics — into a multivariate DoE framework could yield a more holistic optimisation. Furthermore, the choice of a single reference material (CELLINK SKIN) provided a practical benchmark but may have constrained broader applicability; comparisons with multiple commercial or tissue-specific bioinks could enhance the relevance of the findings across a wider range of bioprinting scenarios.

Conclusion

In conclusion, the integration of design of experiment (DoE) techniques with rheological analysis offers a robust methodology for developing bioinks with tailored properties for 3D bioprinting. This study demonstrates the successfully formulation of optimal bioink composition using hyaluronic acid, sodium alginate, and dextran-40, achieving a desired target viscosity and structural integrity.

Future work will be targeted towards investigations into the overall rheological performance of the optimised bioink, its crosslinking properties, and its performance in 3D bioprinting scenarios, to further validate its suitability for complex tissue regeneration.

Funding

Funding for research presented here was provided by Canterbury Christ Church University and Health Education England, Kent, Surrey, Sussex (HEE-KSS).

Data availability

Data for experimental runs are presented in this paper and the supplementary info. Minitab®21 was used to create DoE.

Declarations

Conflict of interest No conflicts of interest exist.

Ethical approval Not applicable (no human tissue used in the experiments presented in this paper).

Supplementary Information The online version contains supplementary material available at https://doi.org/10.1007/s10853-025-11076-1.

References

[1] Langer R, Vacanti JP (1993) Tissue engineering. Science. https://doi.org/10.1126/science.8493529

[2] Gao X, Ruzbarsky JJ, Layne JE, Xiao X, Huard J (2024) Stem cells and bone tissue engineering. Life (Basel) 14(3):287. https://doi.org/10.3390/life14030287

[3] Chung C, Burdick JA (2008) Engineering cartilage tissue. Adv Drug Deliv Rev 60(2):243–262. https://doi.org/10.1016/j.addr.2007.08.027

[4] Kaul H, Ventikos Y (2015) On the genealogy of tissue engineering and regenerative medicine. Tissue Eng Part B Rev 21(2):203–217. https://doi.org/10.1089/ten.teb.2014.0285

[5] Gungor-Ozkerim PS, Inci I, Zhang YS, Khademhosseini A, Dokmeci MR (2018) Bioinks for 3D bioprinting: an overview. Biomater Sci 6(5):915–946. https://doi.org/10.1039/c7bm00765e

[6] Decante G, Costa JB, Silva-Correia J, Collins MN, Reis RL, Oliveira JM (2021) Engineering bioinks for 3D bioprinting. Biofabrication 13(3):032001. https://doi.org/10.1088/1758-5090/abec2c

[7] Jawli A, Aldehani W, Nabi G, Huang Z (2024) Tissue-mimicking material fabrication and properties for multiparametric ultrasound phantoms: a systematic review. Bioengineering 11(6):620. https://doi.org/10.3390/bioengineering11060620

[8] Williams DF (2008) On the mechanisms of biocompatibility. Biomaterials 29(20):2941–2953. https://doi.org/10.1016/j.biomaterials.2008.04.023

[9] Schwab A, Levato R, D'Este M, Piluso S, Eglin D, Malda J (2020) Printability and shape fidelity of bioinks in 3D bioprinting. Chem Rev 120(19):11028–11055. https://doi.org/10.1021/acs.chemrev.0c00084

[10] Jo HJ, Kang MS, Kim JM et al (2024) Bioactive ions-loaded bioinks primed for 3dDprinting of artificial tissues. Biomed Mater Dev 2(2):811–833. https://doi.org/10.1007/s44174-023-00151-3

[11] Chimene D, Kaunas R, Gaharwar AK (2020) Hydrogel bioink reinforcement for additive manufacturing: a focused review of emerging strategies. Adv Mater 32(1):1902026. https://doi.org/10.1002/adma.201902026

[12] Williams D, Thayer P, Martinez H, Gatenholm E, Khademhosseini A (2018) A perspective on the physical, mechanical and biological specifications of bioinks and the development of functional tissues in 3D bioprinting. Bioprinting 9:19–36. https://doi.org/10.1016/j.bprint.2018.02.003

[13] Pedroza-González SC, Rodriguez-Salvador M, Pérez-Benítez BE, Alvarez MM, de Santiago GT (2021) Bioinks for 3D bioprinting: a scientometric analysis of two decades of progress. Int J Bioprint. 7(2):333. https://doi.org/10.18063/ijb.v7i2.337

[14] Kaklamani G, Cheneler D, Grover LM, Adams MJ, Bowen J (2014) Mechanical properties of alginate hydrogels manufactured using external gelation. J Mech Behav Biomed Mater 36:135–142. https://doi.org/10.1016/j.jmbbm.2014.04.013

[15] Marques CF, Diogo GS, Pina S, Oliveira JM, Silva TH, Reis RL (2019) Collagen-based bioinks for hard tissue engineering applications: a comprehensive review. J Mater Sci: Mater Med 30(3):32. https://doi.org/10.1007/s10856-019-6234-x

[16] Yang J, He H, Li D, Zhang Q, Xu L, Ruan C (2023) Advanced strategies in the application of gelatin-based bioink for extrusion bioprinting. Bio-des Manuf 6(5):586–608. https://doi.org/10.1007/s42242-023-00236-4

[17] Burdick JA, Prestwich GD (2011) Hyaluronic acid hydrogels for biomedical applications. https://doi.org/10.1002/adma.201003963. Accessed 3 March 2025

[18] Arif ZU, Khalid MY, Noroozi R, Sadeghianmaryan A, Jalalvand M, Hossain M (2022) Recent advances in 3D-printed polylactide and polycaprolactone-based biomaterials for tissue engineering applications. Int J Biol Macromol 218:930–968. https://doi.org/10.1016/j.ijbiomac.2022.07.140

[19] Cui L, Tong W, Zhou H, Yan C, Chen J, Xiong D (2021) PVA-BA/PEG hydrogel with bilayer structure for biomimetic articular cartilage and investigation of its biotribological and mechanical properties. J Mater Sci 56(5):3935–3946. https://doi.org/10.1007/s10853-020-05467-9

[20] Mendoza-Cerezo L, Jesús MRR, Macías-García A, Marcos-Romero AC, Díaz-Parralejo A (2023) Evolution of bioprinting and current applications. Int J Bioprint. 9(4):742. https://doi.org/10.18063/ijb.742

[21] Paxton N, Smolan W, Böck T, Melchels F, Groll J, Jungst T (2017) Proposal to assess printability of bioinks for extrusion-based bioprinting and evaluation of rheological properties governing bioprintability. Biofabrication 9(4):044107. https://doi.org/10.1088/1758-5090/aa8dd8

[22] Kiyotake EA, Douglas AW, Thomas EE, Nimmo SL, Detamore MS (2019) Development and quantitative characterization of the precursor rheology of hyaluronic acid

hydrogels for bioprinting. Acta Biomater 95:176–187. https://doi.org/10.1016/j.actbio.2019.01.041

[23] Galocha-León C, Antich C, Voltes-Martínez A et al (2025) Human mesenchymal stromal cells-laden crosslinked hyaluronic acid-alginate bioink for 3D bioprinting applications in tissue engineering. Drug Deliv Transl Res 15(1):291–311. https://doi.org/10.1007/s13346-024-01596-9

[24] Butler HM, Naseri E, MacDonald DS, Tasker RA, Ahmadi A (2021) Investigation of rheology, printability, and biocompatibility of N, O-carboxymethyl chitosan and agarose bioinks for 3D bioprinting of neuron cells. Materialia. https://doi.org/10.1016/j.mtla.2021.101169

[25] Yang Y, Jia Y, Yang Q, Xu F (2022) Engineering bio-inks for 3D bioprinting cell mechanical microenvironment. Int J Bioprint. 9(1):632. https://doi.org/10.18063/ijb.v9i1.632

[26] Bercea M (2023) Rheology as a tool for fine-tuning the properties of printable bioinspired gels. Molecules 28(6):2766. https://doi.org/10.3390/molecules28062766

[27] Pössl A, Hartzke D, Schmidts TM, Runkel FE, Schlupp P (2021) A targeted rheological bioink development guideline and its systematic correlation with printing behavior. Biofabrication 13(3):035021. https://doi.org/10.1088/1758-5090/abde1e

[28] Heathman TRJ, Webb WR, Han J et al (2014) Controlled production of poly (3-hydroxybutyrate-co-3-hydroxyhexanoate) (PHBHHx) nanoparticles for targeted and sustained drug delivery. J Pharm Sci 103(8):2498–2508. https://doi.org/10.1002/jps.24035

[29] Petta D, D'Amora U, Ambrosio L, Grijpma DW, Eglin D, D'Este M (2020) Hyaluronic acid as a bioink for extrusion-based 3D printing. Biofabrication 12(3):032001. https://doi.org/10.1088/1758-5090/ab8752

[30] Schmid R, Schmidt SK, Detsch R et al (2022) A new printable alginate/hyaluronic acid/gelatin hydrogel suitable for biofabrication of in vitro and in vivo metastatic melanoma models. Adv Funct Mater 32(2):2107993. https://doi.org/10.1002/adfm.202107993

[31] Zidarič T, Milojević M, Gradišnik L, StanaKleinschek K, Maver U, Maver T (2020) Polysaccharide-based bioink formulation for 3D bioprinting of an in vitro model of the human dermis. Nanomaterials (Basel) 10(4):733. https://doi.org/10.3390/nano10040733

[32] Cavallo A, Al Kayal T, Mero A et al (2023) Marine collagen-based bioink for 3D bioprinting of a bilayered skin model. Pharmaceutics 15(5):1331. https://doi.org/10.3390/pharmaceutics15051331

[33] Gervasi V, Cullen S, McCoy T, Crean A, Vucen S (2019) Application of a mixture DOE for the prediction of formulation critical temperatures during lyophilisation process optimisation. Int J Pharm 572:118807. https://doi.org/10.1016/j.ijpharm.2019.118807

[34] Avramova T, Vasileva D, Peneva T (2024) An overview of the basic concepts and terms related to manufacturing process capability evaluation. AIP Conf Proc 3104:020011. https://doi.org/10.1063/5.0198835